Mineralogical Magazine, February 2004, Vol. 68(1), pp. 167–175

New insight into the crystal structure of orthorhombic edingtonite: evidence for a split Ba site

G. D. GATTA* AND T. BOFFA BALLARAN

Bayerisches Geoinstitut, Universitaet Bayreuth, Universitaet Strasse 30, D-95447 Bayreuth, Germany

ABSTRACT

Orthorhombic edingtonite has been found coexisting with tetragonal edingtonite in a specimen from Ice River, British Columbia, Canada.

We report data on the composition and crystal structure of the orthorhombic sample. Lattice parameters are: a = 9.5341(6), b = 9.6446(6), c = 6.5108(7) Å, V = 598.68(8) Å^3. The crystal structure was refined in space group $P\ 2_12_12$ to R_1 = 1.8% using 879 observed reflections. For the first time, evidence for splitting of the extra-framework Ba site in two different sites (Ba1, Ba2), ~0.37 Å apart, is demonstrated. A comparison with the published crystal structures of tetragonal and orthorhombic edingtonite is made.

The present result supports the suggestion that the two edingtonite phases are a consequence of different nucleation phenomena and not different physicochemical conditions.

KEYWORDS: fibrous zeolite, orthorhombic edingtonite, single-crystal X-ray diffraction, crystal structure, Ba-split site.

Introduction

EDINGTONITE belongs to the 'fibrous zeolites' group, with an ideal chemical composition of $Ba_2Al_4Si_6O_{20}{\cdot}8H_2O$ (Gottardi and Galli, 1985; Armbruster and Gunter, 2001). The crystal structure of edingtonite from Böhlet Mine, Sweden, was originally determined by Taylor and Jackson (1933) in space group $P\bar{4}2_1m$. The authors described the specimen as tetragonal, but they did not exclude orthorhombic symmetry, given the high uncertainties of the lattice constants obtained and the low quality of the structural refinements at that time. Galli (1976) reinvestigated the crystal structure of a Swedish edingtonite from Böhlet Mine in space group $P2_12_12$ using single-crystal X-ray diffraction (XRD) and Kvick and Smith (1983) refined the crystal structure of an orthorhombic specimen from New Brunswick, Canada, by single-crystal neutron diffraction; they were able to determine all hydrogen sites. Mazzi *et al.* (1984) reported the crystal structure of two tetragonal edingtonites, from Ice River, Canada, and from Old Kilpatrick, Dumbartonshire, Scotland. The lattice was tetragonal within the experimental error with space group $P\bar{4}2_1m$, which is the topological symmetry of this framework type and also the maximum possible symmetry for this framework (Gottardi and Galli, 1985). At the same time, Grice *et al.* (1984) reported the occurrence of orthorhombic edingtonite from the same locality (Ice River, Canada). Cell parameters, optical properties and chemical analysis were reported, as well as two common twinning laws: lamellar (110) and penetration [001] with individuals at 90º.

The thermal behaviour of orthorhombic edingtonite was investigated by Belitsky *et al.* (1986), Ståhl and Hanson (1998) and Goryainov *et al.* (2003). A $P2_12_12 \rightarrow P112$ phase transition due to a change of the H-position has been observed at low temperature (Belitsky *et al.*, 1986; Goryainov *et al.*, 2003). High-temperature dehydration of orthorhombic edingtonite was investigated by Ståhl and Hanson (1998). The structural refine-

* E-mail: diego.gatta@uni-bayreuth.de
DOI: 10.1180/0026461046810178

ments showed a continuous loss of water up to 660 K, but no phase transformation to tetragonal symmetry has been observed. The crystal structure breaks down rapidly above 660 K. The high-pressure behaviour of orthorhombic edingtonite was studied up to 6 GPa by Goryainov *et al.* (2003) with Raman spectroscopy. No phase transition has been observed within the pressure range investigated. The main difference between tetragonal and orthorhombic edingtonite is the (Si,Al)-ordering in the tetrahedra which reduces the lattice symmetry from $P\bar{4}2_1m$ to $P2_12_12$. The (Si,Al)-framework of this fibrous zeolite consists of tetrahedral chains (topological symmetry $P\bar{4}2_1m$) running along [001] (Fig. 1). The fundamental polyhedral unit for these chains is the "4 = 1 secondary building unit (SBU)" (Baerlocher *et al.*, 2001) (Fig. 1). The framework encloses two systems of channels: 8-ring channels along [001] and 8-ring channels along [110] (Fig. 1). The extra-framework cations and water molecules lie in these channels. In both tetragonal and orthorhombic edingtonite there is only one extra-framework cation site occupied by Ba (minor amounts of K, Na, Sr and Ca were also observed) and two independent water molecule sites. Six framework oxygens and four water molecules constitute the Ba-coordination polyhedron.

In tetragonal edingtonite (Mazzi *et al.*, 1984) the Ba site is split into two sites ~0.46 Å apart. Most Ba^{2+} (up to 90%) is at the Ba1 site and a minor amount (<5%) is at the Ba2 site; the sum of the occupancy factors of the two sites is <100%. In contrast, structural refinements of orthorhombic edingtonites (Galli, 1976; Kvick and Smith, 1983) do not indicate splitting of the Ba site. There are no clear explanations for this difference in Ba topology between tetragonal and orthorhombic edingtonite. The discovery of orthorhombic edingtonite in a sample from Ice River, coexisting with the tetragonal sample used for the refinement by Mazzi *et al.* (1984), gave us the opportunity to reinvestigate the crystal structure of orthorhombic edingtonite in order to clarify the behaviour of Ba in both structures variants.

Experimental methods

The edingtonite specimen studied here comes from the alkaline complex at Ice River, Kootenay District, British Columbia, Canada. The acicular/prismatic crystals (average size: $0.6 \times 0.6 \times 3$ mm) of orthorhombic and tetragonal edingtonite are found in the hydrothermal veins of the nepheline syenite, associated with natrolite (Grice and Gault, 1984). E. Galli and E. Passaglia from the University of Modena (Italy) kindly provided samples (fibrous aggregate crystals nominally tetragonal). The crystals of the two symmetry variants are adjacent without any evidence of intergrowth and distinction is difficult by optical microscope under polarized light, therefore only XRD of several single crystals made the separation of the two crystal types possible. Electron microprobe analysis of the same crystal used for the XRD experiment was performed using a fully automated CAMECA SX-50 microprobe, operating in WDS mode. Major and minor elements were determined at 15 kV accelerating voltage and 10 nA beam current with a counting time of 20 s. Since this mineral loses water when heated, the crystal was mounted in epoxy resin and a defocused beam was used to minimize loss of water due to the electron bombardment. The standards employed were: albite (Al, Si, Na), microcline (K), anorthite (Ca), baryte (Ba), celestite (Sr), diopside (Mg). The crystal was found to be homogeneous within the analytical error. The chemical content obtained by averaging six point analyses gives Na_2O 0.07%, K_2O 0.25%, CaO 0.01%, MgO <0.01%, BaO 29.42%, Al_2O_3 19.76%, SiO_2 37.44%, H_2O 13.04% (by difference). The chemical formula, on the basis of 28 oxygen atoms, is $(Ba_{1.96}K_{0.06}Na_{0.02})Al_{3.95}Si_{6.35}O_{20}\cdot 7.37\ H_2O$. This chemical composition is very similar to that reported by Grice *et al.* (1984) for orthorhombic edingtonite of the same locality and to the chemical formula of tetragonal edingtonite from Ice River published by Mazzi *et al.* (1984).

Accurate lattice parameters were determined at T = 293 K using a Huber four-circle diffractometer (not-monochromatized Mo-$K\alpha$) using

FIG. 1. (*facing page*) Projection of the crystal structure of orthorhombic edingtonite viewed *(a)* down [001], and (*b*) viewed down [110], showing the Secondary Building Unit chains along [001]. The two channel systems and the extra-framework population are shown. The large spheres represent cation sites, whereas the small spheres represent the oxygen (dark) and hydrogen (white) sites of the water molecules. Structure visualization by DIAMOND program (Pennington, 1999). $\varphi° = [180° - (O1-O1-O1)°]/2$.

a

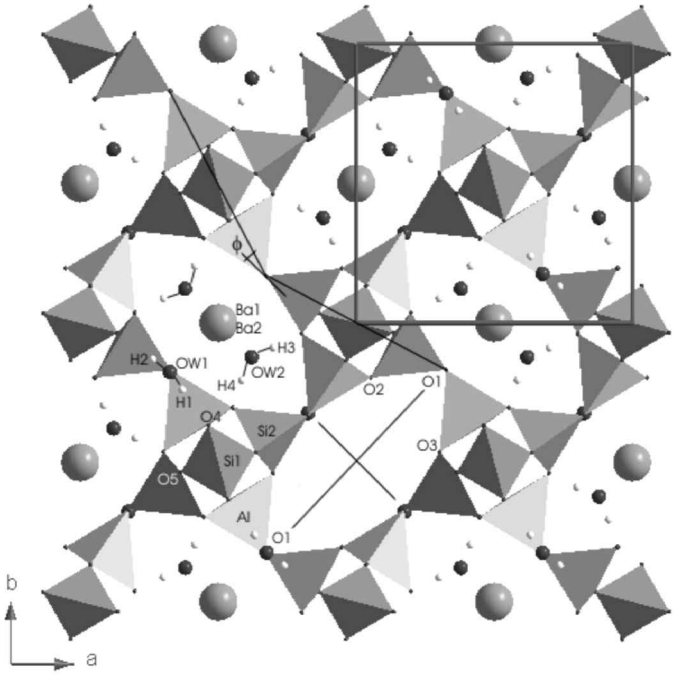
ϕ
Ba1
Ba2
H3
H2
OW1
OW2
H4
H1
O4
Si2
O2
O1
O3
Si1
O5
Al
O1
b
a

b

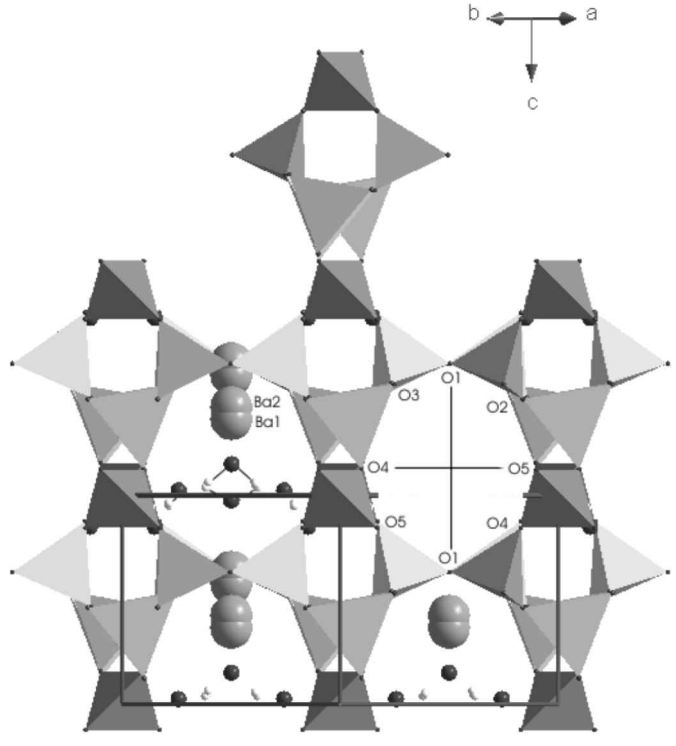
b
a
c
O1
O3
O2
Ba2
Ba1
O4
O5
O5
O4
O1

eight-position centering of 26 Bragg reflections (King and Finger, 1979; Angel *et al.*, 2000). The centering procedure and vector-least-squares refinement of the unit-cell parameters were performed using the SINGLE software (Ralph and Finger, 1982; Angel *et al.*, 2000), giving metrically orthorhombic cell parameters: a = 9.5341(6), b = 9.6446(6), c = 6.5108(7) Å, V = 598.68(8) Å^3. Intensity data were collected on a Nonius-CAD4 diffractometer (graphite-monochromated Mo-$K\alpha$ X-radiation) operated at 50 kV and 40 mA. Details of the data collection are reported in Table 1. A total of 1744 reflections was collected in the range $1 < \theta < 30°$, of which 1478 unique reflections had $F_o > 4\sigma(F_o)$. After Lorentz, polarization and empirical absorption corrections, based on the method of North *et al.* (1968), the discrepancy factor for symmetry-related reflections was R_{int} = 0.021 (Table 1).

Structure refinement

The structure refinement was carried out at first with isotropic displacement parameters in space group $P2_12_12$ using the SHELXL-97 package (Sheldrick, 1997), starting from the atomic coordinates of Kvick and Smith (1983). Neutral atomic scattering factor values of Si, Al, Ba, O and H from the *International Tables for X-ray Crystallography* (Ibers and Hamilton, 1974) were used. Isotropic extinction correction has been applied according to the Larson method (1970), as implemented in SHELXL-97 (Sheldrick, 1997). Taking into account that the crystal structure is non-centrosymmetric, merohedral twinning by the pseudo-centre of symmetry and the correct set-up of the 'absolute structure' (correct, inverse) was considered in the structural refinements according to the Flack test (Flack, 1983). The Flack test confirmed a correct structure set-up and the absence of racemic/merohedral twinning (Table 1). In the first least-square cycles, the scale factor and the occupancies of the Ba sites were not simultaneously refined, since they appeared strongly correlated. All hydrogen atoms were located by difference-Fourier map analysis and their coordinates appeared close to those found by Kvick and Smith (1983) by neutron diffraction. Site parameters of the hydrogen atoms (x, y, z, U_{iso}) were then fixed to values reported by Kvick and Smith (1983); the occupancy factors were fixed to equal the refined occupancy factors of the respective water oxygen atoms (Table 2). The structure refinement conducted with only one Ba site, as in previous work (Galli, 1976; Kvick and Smith, 1983), produced a residual peak in the final difference-Fourier synthesis of ~2.5 e^-/Å^3 at ~0.37 Å from the Ba position, as shown in the electron density map in Fig. 2. A further refinement with the Ba-site split into Ba1 and Ba2 sites resulted in an improvement of the agreement index. At the end of the last refinement, no peak larger than 0.8 e^-/Å^3 was present in the final difference-Fourier map. The final least-square cycles were conducted with anisotropic thermal parameters, but isotropic displacement parameters were used for the poorly occupied Ba2 site and the hydrogen atoms (Table 2). The final agreement index (R_1) was 0.018 for 99 refined parameters and 879 observed reflections (Table 1). A structure refinement performed using the ionic scattering curves did not provide significantly different results.

Observed and calculated structure factors can be obtained from the authors upon request (or from the Principal Editor). Positional and displacement parameters are reported in Table 2. Relevant bond lengths and geometrical parameters are listed in Tables 3 and 4.

TABLE 1. Details of data collection and refinement of orthorhombic edingtonite from Ice River (Canada).

Crystal size (μm)	200 × 110 × 70
Cell parameters	a = 9.5341(6) Å
	b = 9.6446(6) Å
	c = 6.5108(7) Å
	V = 598.68(8) Å^3
Z	1
T (K)	293
Radiation	Mo-$K\alpha$
μ (Mo-$K\alpha$) (cm^{-1})	38.4
ρ_{calc} (g cm^{-3})	2.816
Scan speed (°/min)	3.28
ω-scan width (°)	0.7
Space group	$P2_12_12$
No. measured reflections	1744
No. unique refl. with $F_o > 4\sigma(F_o)$	1478
No. 'observed' reflections	879
No. refined parameters	99
Flack x parameter	0.0005
Extinction factor	0.0034
R_{int}	0.021
R_1 (F)	0.018
R_1 (F) for 1478 reflections	0.021
R_1 (F) for all reflections	0.036

$R_{int} = \Sigma|F_{obs}^2 - F_{obs}^2(mean)|/\Sigma[F_{obs}^2]$;
$R_1 = \Sigma(|F_{obs}| - |F_{calc}|)/\Sigma|F_{obs}|$.

TABLE 2. Refined positional and displacement parameters (Å^2) for orthorhombic edingtonite.

Site	x	y	z	Site occup.	U_{11}	U_{22}	U_{33}	U_{12}	U_{13}	U_{23}	U_{eq}/U_{iso}
Ba1	0.5	0.0	0.6343(5)	0.89(1)	0.0124(1)	0.0148(2)	0.0188(8)	0.0	0.0	−0.0029(1)	0.0153(3)
Ba2	0.5	0.0	0.5774(24)	0.10(1)							0.0076(13)
Si1	0.0	0.0	−0.0130(1)	1.0	0.0082(4)	0.0086(4)	0.0074(4)	0.0	0.0	−0.0004(7)	0.0081(2)
Si2	−0.1758(1)	0.0939(1)	0.3874(1)	1.0	0.0071(3)	0.0078(3)	0.0076(4)	0.0007(3)	0.0002(3)	0.0009(3)	0.0075(2)
Al	0.0920(1)	0.1716(1)	0.6265(2)	1.0	0.0076(3)	0.0065(3)	0.0074(4)	−0.0003(3)	0.0003(4)	−0.0005(3)	0.0071(2)
O1	0.1735(2)	0.3316(2)	0.6318(4)	1.0	0.0096(9)	0.0097(8)	0.0150(10)	0.0020(10)	−0.0021(10)	−0.0025(7)	0.0114(4)
O2	−0.0528(2)	0.1960(2)	0.4666(4)	1.0	0.0125(9)	0.0148(11)	0.0136(11)	0.0015(9)	−0.0042(8)	−0.0026(9)	0.0137(5)
O3	0.1979(2)	0.0379(2)	0.5384(4)	1.0	0.0142(10)	0.0093(10)	0.0154(11)	−0.0038(8)	−0.0032(9)	0.0027(8)	0.0130(5)
O4	0.0361(2)	0.1341(2)	0.8763(4)	1.0	0.0199(11)	0.0105(9)	0.0122(9)	0.0020(10)	0.0034(9)	−0.0008(7)	0.0142(4)
O5	−0.1354(2)	0.0349(2)	0.1566(4)	1.0	0.0112(9)	0.0175(11)	0.0127(10)	−0.0016(8)	0.0022(8)	0.0018(8)	0.0138(5)
OW1	0.1752(4)	0.3235(4)	0.1501(7)	0.81(1)	0.0390(22)	0.0364(21)	0.0282(22)	−0.0125(18)	0.0111(18)	−0.0160(17)	0.0345(12)
H1*	0.1308	0.2604	0.0562	0.81							0.0400
H2*	0.2374	0.3694	0.0635	0.81							0.0400
OW2	0.3794(5)	0.1222(5)	-0.0237(8)	0.90(1)	0.0496(29)	0.0453(27)	0.0584(30)	−0.0205(22)	0.0158(23)	−0.0127(21)	0.0511(17)
H3*	0.3005	0.0884	0.0494	0.90							0.0400
H4*	0.4151	0.2044	0.0377	0.90							0.0400

* x, y, z, site occupancy and U_{iso} fixed (see text)

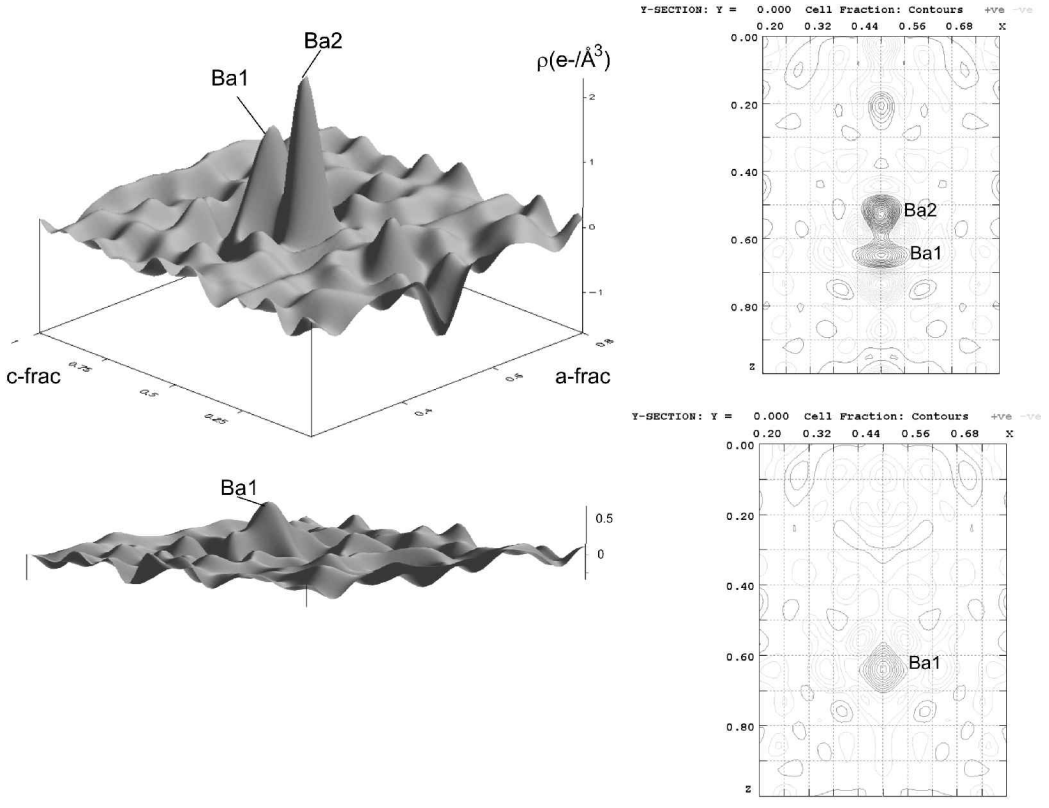

FIG. 2. 2D and 3D F_{obs}-F_{calc} electron density maps; without considering the Ba2 site in the refinement (upper) and considering the Ba2 site (lower). In the first case, the most intensive residual peak is ~2.5 e^-/Å^3 and is located on the Ba2-site position; in the latter case it is <0.8 e^-/Å^3 and it is located on the Ba1-site position, as expected for heavy atoms. For comparison, the 3D maps are plotted with the same ordinate scale. Maps drawn using MAPVIEW and CONTOUR in the *WinGX* package (Farrugia, 1999).

Discussion

The crystal structures of orthorhombic edingtonite from Böhlet Mine, Sweden, and New Brunswick, Canada, refined by Galli (1976) and Kvick and Smith (1983), respectively, have only one Ba site. The sample investigated in this study has coordinates of the framework and extra-framework atoms (Table 2) very close to those found in the previous work. However, we have found strong evidence for the existence of a split Ba site analogous to that reported by Mazzi *et al.* (1984) for tetragonal edingtonite. Special care was, therefore, devoted to address the tetrahedral Si/Al-ordering, which determines the edingtonite symmetry, and to the location of the split Ba sites (Ba1, Ba2). The Si/Al-ordering among the tetrahedra demonstrates the effective general orthorhombic symmetry of this specimen. Al and Si are fully ordered into the Al, Si1 and Si2 sites, as confirmed by Al–O, Si1–O and Si2–O mean distances of 1.739, 1.618 and 1.625 Å, respectively (Table 3). The geometrical relationships between the (Si,Al)-chains themselves and the channel systems morphology were also analysed. The angle between the adjacent [001]-chains, here defined as $\varphi° = [180° - (O1-O1-O1)°]/2$ (Fig. 1*a*) is 17.55(8)° (Table 4). The channel ellipticity has been calculated as the ratio between the smaller 'free diameter', the effective pore width based on oxygen radius of 1.35 Å (Baerlocher *et al.*, 2001), and the larger one: $\varepsilon_{[001]}$ = O1–O1(short)/O1–O1(long) for the 8-ring channel along [001] is 0.31; $\varepsilon_{[110]}$ = O4–O5(long)/O1–O1 for the 8-ring channel along [110] (Fig. 1) is 0.72. From the coordinates reported by Mazzi *et al.* (1984),

TABLE 3. Selected interatomic distances (Å).

Ba1 – O1 (× 2)	2.894(3)
Ba1 – O2 (× 2)	3.046(2)
Ba1 – O3 (× 2)	2.970(2)
Ba1 – OW1 (× 2)	2.767(5)
Ba1 – OW2 (× 2)	2.769(5)
Ba2 – O1 (× 2)	2.689(8)
Ba2 – O2 (× 2)	2.989(3)
Ba2 – O3 (× 2)	2.915(3)
Ba2 – OW1 (× 2)	2.972(10)
Ba2 – OW2 (× 2)	3.075(14)
OW1 – H1	0.961(4)
OW1 – H2	0.930(4)
OW2 – H3	0.949(4)
OW2 – H4	0.950(4)
Si1 – O4 (× 2)	1.608(2)
Si1 – O5 (× 2)	1.629(2)
<Si2 – O>	1.618
Si2 – O1	1.610(2)
Si2 – O2	1.616(2)
Si2 – O3	1.621(2)
Si2 – O5	1.652(3)
<Si2 – O>	1.625
Al – O1	1.729(2)
Al – O2	1.745(3)
Al – O3	1.735(2)
Al – O4	1.749(3)
<Al – O>	1.739

TABLE 4. Relevant structural parameters for orthorhombic edingtonite.

Si1-tetrahedron	
O4 – Si1 – O4(°)	112.73(19)
O4 – Si1 – O5(°) (× 2)	108.34(12)
O4 – Si1 – O5(°) (× 2)	108.73(11)
O5 – Si1 – O5(°)	109.96(17)
Si2 – tetrahedron	
O1 – Si2 – O2(°)	113.58(13)
O1 – Si2 – O3(°)	106.33(12)
O1 – Si2 – O5(°)	106.93(13)
O2 – Si2 – O3(°)	112.23(13)
O2 – Si2 – O5(°)	109.30(13)
O3 – Si2 – O5(°)	108.19(12)
Al-tetrahedron	
O1 – Al – O2(°)	104.30(12)
O1 – Al – O3(°)	114.12(12)
O1 – Al – O4(°)	107.64(13)
O2 – Al – O3(°)	111.32(12)
O2 – Al – O4(°)	109.95(12)
O3 – Al – O4(°)	109.34(11)
Channel [110]	
O1↔O1 (Å) ('free diameter')	3.811(5)
O4↔O5 (Å)	2.739(7)
O5↔O4 (Å)	1.777(5)
O3↔O2(Å)	2.025(6)
ε [110]	0.72
Channel [001]	
O1↔O1 (Å)	6.226(8)
O1↔O1 (Å)	1.936(7)
O3↔O2 (Å)	0.798(5)
ε [001]	0.31
φ(°)	17.56(9)

'free diameter', ε and φ are defined in the text

we calculate that for the tetragonal edingtonite $\varphi^{\circ} \approx 17.01^{\circ}$, $\varepsilon_{[001]} \approx 0.33$ and $\varepsilon_{[110]} \approx 0.71$, i.e. very similar values. Another factor which may play a role in determining the symmetry of edingtonite is the impurity content of the specimen. Hey (1934) and Taylor (1935) suggested that a high impurity content stabilizes the tetragonal with respect to the orthorhombic symmetry. However, the amount of K^+ in both tetragonal (0.11 a.p.f.u. of K^+, Mazzi *et al.*, 1984) and orthorhombic specimens (0–0.06 a.p.f.u. of K^+, Belitsky *et al.*, 1986; Galli, 1976; Grice *et al.*, 1984; Kvick and Smith, 1983; this study), are very similar, therefore their amount cannot be responsible for the different symmetry.

Our structural data confirm that the orthorhombic edingtonite from Ice River also has the Ba^{2+} site split into two sub-sites ~0.37 Å apart (Fig. 3). We cannot exclude the possibiliy that the quality of previously published datasets for orthorhombic edingtonite may have been insufficient to locate a very poorly occupied Ba2 site. Galli (1976) reports there to be "no significant residual" for the final difference-Fourier synthesis; Kvick and Smith (1983) quantified the largest residual peak as <4% of any oxygens atom; Belitsky *et al.* (1986) did not report any information about residual peaks in the difference-Fourier synthesis. As in tetragonal edingtonite (Mazzi *et al.*, 1984), the possibility that other cations (Na, Ca, K, Sr) could cause the splitting of the Ba site by concentrating into the Ba2 site can be excluded given the negligible content of such impurities. Refinement trials with the K scattering curve for the Ba2 site led to excessive occupancy factors. It appears, therefore, that K is distributed between the two split sites. However, given the similar bond distances of K and Ba in the edingtonite extra-framework configuration it is impossible to determine if K is concentrated preferentially in one of the two split sites.

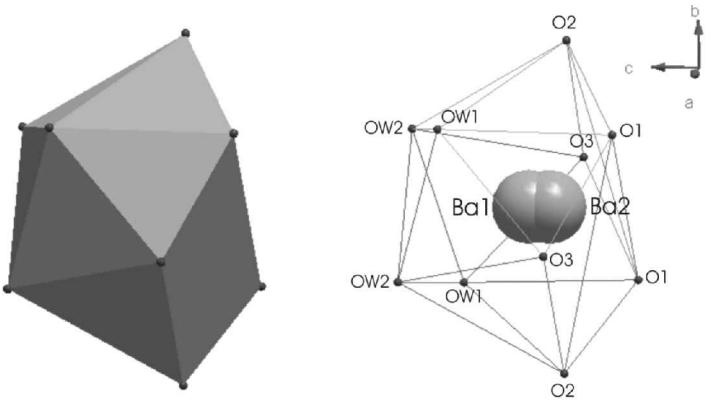

FIG. 3. Ba-coordination polyhedron (closed faces on the left, open faces on the right).

The sum of the occupancy factors of the two sites in our structure is close to 100%: the occupancy of tha Ba1 site is ~89%, whereas the occupancy of the Ba2 site is ~10% (Table 2). On the contrary, the sum of the occupancies of the two Ba sites for the tetragonal edingtonite on the same specimen is <100% (~94%; Mazzi *et al.*, 1984). Less than full occupancy of the only Ba site (~97%) was also observed by Kvick and Smith (1983) for orthorhombic edingtonite.

Mazzi *et al.* (1984) proposed a possible explanation of the site splitting observed for the tetragonal edingtonite. The splitting of the Ba site and the low occupancy of the Ba2 site may be due to the water-molecule sites not being fully occupied. The anomalous set of distances between the Ba1 site and framework/water molecules oxygens, which form the Ba-coordination sphere, may be significant in this respect. In both our and Mazzi's sample the distances between Ba1-framework oxygens (Ba1–O1, Ba1–O2, Ba1–O3) are longer than the distances between Ba1 and water molecules (Ba1–OW1, Ba1–OW2) (Table 3). This configuration is the opposite of that normally found in zeolites and appears to be energetically unfavourable. Our refined occupancies of the H_2O sites, 81% for OW1 and 90% for OW2, are very similar to those reported by Kvick and Smith (1983) (84% for OW1 and 90% for OW2). This similarity suggests that the different topological configuration for the Ba site observed between the two orthorhombic specimens is not only a consequence of the water occupancy factors, but may be due to a combined effect of the Ba content and water occupancies, given similar bond-distance values.

The coexistence of tetragonal (disordered) and orthorhombic (fully ordered) edingtonite strongly supports the suggestion proposed by Mazzi *et al.* (1984) that the formation of edingtonite having two different symmetries is not due to different physicochemical conditions. The hydrothermal genesis of these zeolites is restricted to temperatures of ~350–500 K (Mazzi *et al.*, 1984; Gottardi and Galli, 1985; Ghobarkar and Schaef, 1997). Although the effect of temperature, growth speed and/or cooling process on the Si/Al-ordering of this zeolite is still unknown, it is unlikely that in such a small temperature range, there would be distinct stability fields for orthorhombic and tetragonal phases. As suggested by Mazzi *et al.* (1984), it would seem more likely that the two types of edingtonite are due, in fact, to different nucleation phenomena.

Acknowledgements

Thanks are due to E. Galli and E. Passaglia (University of Modena, Italy) for the sample of edingtonite from Ice River. This work was supported financially by the Sofia Kovalevskaja award to T. Boffa Ballaran.

References

Angel, R.J., Downs, R.T. and Finger, L.W. (2000) High-Temperature–High-Pressure Diffractometry. Pp. 559-596 in: *High-Temperature and High-Pressure Crystal Chemistry* (R.M. Hazen and R.T. Downs, edtiors). Reviews in Mineralogy and Geochemistry, **41**. Mineralogical Society of America and Geochemical Society, Washington, D.C., USA.

Armbruster, T. and Gunter, M.E. (2001) Crystal structures of natural zeolites. Pp. 1-57 in: *Natural Zeolites: Occurrence, Properties, Application* (D.L. Bish and D.W. Ming, editors). Reviews in Mineralogy and Geochemistry, **45**. Mineralogical Society of America and Geochemical Society, Washington, D.C., USA.

Baerlocher, Ch., Meier, W.M. and Olson, D.H. (2001) *Atlas of Zeolite Framework Types*, 5th edition. Elsevier, Amsterdam, Netherlands, 302 pp.

Belitsky, I.A., Gabuda, S.P., Joswig, W. and Fuess, H. (1986) Study of the structure and dynamics of water in the zeolite edingtonite at low temperature by neutron diffraction and NMR-spectroscopy. *Neues Jahrbuch für Mineralogie Monatshefte*, 541–551.

Farrugia, L.J. (1999) *WinGX* suite for small-molecule single-crystal crystallography. *Journal of Applied Crystallography*, **32**, 837–838.

Flack, H.D. (1983) On enantiomorph-polarity estimation. *Acta Crystallographica*, **A39**, 876–881.

Galli, E. (1976) Crystal structure refinement of edingtonite. *Acta Crystallographica*, **B32**, 1623–1627.

Ghobarkar, H. and Schaef, O. (1997) Hydrothermal synthesis and morphology determination of thomsonite and edingtonite. *Crystal Research and Technology*, **32**, 653–657.

Goryainov, S.V., Kursonov, A.V, Miroshnichenko, Yu.M., Smirnov, M.B. and Kabanov, I.S. (2003) Low-temperature anomalies of infrared band intensities and high-pressure behaviour of edingtonite. *Microporous and Mesoporous Materials*, **61**, 283–289.

Gottardi, G. and Galli, E. (1985) *Natural Zeolites*. Springer-Verlag, Berlin, 409 pp.

Grice, J.D., Gault, R.A. and Ansell, H.G. (1984) Edingtonite: the first two Canadian occurrences. *The Canadian Mineralogist*, **22**, 253–258.

Hey, M.H. (1934) Studies on the zeolites. VI. Edingtonite. *Mineralogical Magazine*, **23**, 483–494.

Ibers, J.A. and Hamilton, W.C., editors (1974) *International Tables for X-ray Crystallography*, vol. IV, Kynoch, Birmingham, UK.

King, H.E. and Finger, L.W. (1979) Diffracted beam crystal centering and its application to high-pressure crystallography. *Journal of Applied Crystallography*, **12**, 374–378.

Kvick, A. and Smith, J.V. (1983) A neutron diffraction study of the zeolite edingtonite. *Journal of Chemical Physics*, **79**, 2356–2362.

Larson, A.C. (1970) *Crystallographic Computing* (F.R. Ahmed, S.R. Hall and C.P. Huber, editors). Munksgaard, Copenhagen, Denmark, pp. 291–294.

Mazzi, F., Galli, E. and Gottardi, G. (1984) Crystal structure refinement of two tetragonal edingtonites. *Neues Jahrbuch für Mineralogie Monatshefte*, 373–382.

North, A.C.T., Phillips, D.C. and Mathews, F.S. (1968) A semiempirical method of absorption correction. *Acta Crystallographica*, **A24**, 351–359.

Pennington, W.T. (1999) DIAMOND-Visual Crystal Software Information System. *Journal of Applied Crystallography*, **32**, 1028–1029.

Ralph, R.L. and Finger, L.W. (1982) A computer program for refinement of crystal orientation matrix and lattice constants from diffractometer data with lattice symmetry constraints. *Journal of Applied Crystallography*, **15**, 537–539.

Sheldrick, G.M. (1997) *SHELX-97. Programs for Crystal Structure Determination and Refinement*. Univeristy of Goettingen, Germany.

Ståhl, K. and Hanson, J.C. (1998) An in situ study of the edingtonite dehydration process from X-ray synchrotron powder diffraction. *European Journal of Mineralogy*, **10**, 221–228.

Taylor, W.H. (1935) An X-ray examination of substituted edingtonites. *Mineralogical Magazine*, **24**, 208–220.

Taylor, W.H. and Jackson, R. (1933) The structure of edingtonite. *Zeitschrift für Kristallographie*, **86**, 53–64.

[*Manuscript received 11 August 2003: revised 17 December 2003*]